Femtosecond pulse distortion in GaAs quantum wells and its effect on pump-probe or four-wave-mixing experiments

D. S. Kim,* J. Shah, D. A. B. Miller, T. C. Damen, and A. Vinattieri
AT&T Bell Laboratories, Holmdel, New Jersey 07733

Wilfred Schäfer
Hochstleistungsrechenzentrum, Forschungszentrum Jülich, W-5170 Jülich, Federal Republic of Germany

L. N. Pfeiffer
AT&T Bell Laboratories, Murray Hill, New Jersey 07974

(Received 5 July 1994; revised manuscript received 19 September 1994)

We show that a low-intensity femtosecond pulse is severely distorted while propagating through a relatively thin ($\approx$6300 Å) GaAs multiple-quantum-well sample near the exciton resonance at low temperatures. This pulse distortion depends critically on the dephasing time T_2, the total thickness l, detuning, and inhomogeneous broadening. In thinner, high-quality samples ($l<3000$ Å, exciton linewidth <1 meV), the distortion is smaller and free-induction-decay-like. An interferometric measurement reveals the existence of well-defined nodes at which the envelope function changes its sign, demonstrating that the source of the pulse distortion is the reradiation of the induced dipoles. While the effects of this pulse distortion on pump-probe or four-wave-mixing experiments are relatively small for samples with $l<3000$ Å, samples with $l>6000$ Å are strongly affected.

I. INTRODUCTION

Many interesting femtosecond phenomena near the exciton resonances in semiconductor superlattices are strongly influenced by the interplay between the following three coherent fields: the incident field (E_0), the interaction-induced field created by Coulomb interaction between coherent excitons ($E_{\rm II}$), and the *reradiation of the coherent excitonic polarization* into the forward direction (E_R) (Fig. 1). This is essentially because with excitons at low temperature, the following condition: $T_2 \gg t_p$(T_2, dephasing time: t_p, pulse width) is easily satisfied. Since $E_{\rm II}$ is created by absorption, which is generally described by the imaginary part of the dielectric constant, it is 90° out of phase from the incident field (Fig. 1). Furthermore, it is proportional to the induced polarization and has the same phase. For this reason, it is often called the polarization field or the local field. The relative importance of this induced field is essentially independent of total well thickness l or the propagation distance because of its microscopic or local nature. On the other hand, E_R becomes more and more important as the pulse propagates through the sample, and therefore, this is an effect that is very sensitive to the sample thickness.[6–9] This is a result of causality, so that an exciton at a position $z<l$ feels the reradiation of coherent polarizations between 0 and z, where the propagation direction is z and the pulse enters the sample at $z=0$. The reradiated field is another 90° out of phase from that of the induced dipoles, so that its sign is opposite from the incident field (Fig. 1).

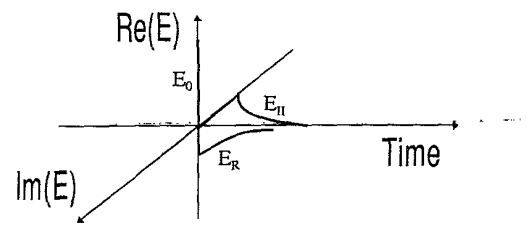

FIG. 1. Schematics of the incident (real, positive, E_0), the interaction induced (imaginary, 90° out of phase $E_{\rm II}$), and the reradiated field (real, negative, 180° out of phase, E_R) inside a semiconductor near an excitonic resonance.

It is clear that in a given experiment [such as pump-probe, four-wave-mixing (FWM) or THz experiments], the roles of E_0, $E_{\rm II}$, and E_R should be carefully considered. Recently, the effect of $E_{\rm II}$ on FWM signal from excitons has been a subject of intense studies, both theoretical and experimental.[1–5] It is now well known that FWM Is dominated by the diffraction of $E_{\rm II}$ at low temperature, which imply $VT_2/\hbar > 1$.[4,5] This results in completely different behaviors in both time-integrated (TI) and time-resolved (TR) FWM from the predictions of the noninteracting two level.

Unlike $E_{\rm II}$, the roles of E_R in most experiments can be negligible provided that the sample is arbitrarily thin, i.e., $\alpha l \ll 1$ where α is the peak absorption coefficient. In some situations, the condition can be somewhat relaxed to $\alpha l < 1$–2. However, many samples used in femtosecond experiments are optically thick, with $\alpha l > 1$ or even $\alpha l \gg 1$. In such cases, the effects of pulse distortion or E_R should be carefully considered.

In the following, we present analytical expressions for

E_{II} and E_R under δ-function excitation, which are appropriate for $\alpha l < 1$ and two-level systems. When $\alpha l > 1$, essential physics remains the same although the expressions are much more complicated, involving convolution of the first Bessel function with the pulse shape, which result in aperiodic oscillations.[6–9] When the sample is optically thin, i.e., $\alpha l < 1$ and assuming $E_0 = \delta(t)$ at resonance, the generally complicated solution can be reduced into the following simplified form:

$$E_{\text{total}}(z<l) = E_0 + E_{II} + E_R \approx \delta(t') + (2iV/\hbar)\theta(t')\exp(-t'/T_2) - \{\alpha z/(2T_2)\}\theta(t')\exp(-t'/T_2) , \quad (1)$$

where $t' = t - z/v$ and v is the propagation velocity. V is an average interaction potential and α is the peak absorption coefficient, whereas $\theta(t)$ is the heaviside step function. E_{II} is "local," and, therefore, exists only inside the semiconductor, whereas reradiation of the induced dipoles creates an electric field outside the semiconductor. Thus, the "exiting" pulse shape is:

$$E(z>l) = \delta(t'') - \alpha l/(2T_2)\theta(t'')\exp(-t''/T_2) , \quad (2)$$

where $t'' = t - l/v - (z-l)/c$ (c, speed of light in the air). The second part of Eq. (2) results from the reradiation of the coherent, induced dipoles of the entire sample, and is often called the free induction decay (FID). It should be noted that Eqs. (1) and (2) are density independent and linear, and are appropriate for resonant excitations at low or modest densities before the Pauli blocking factor becomes important. Thus far, excitons were assumed to be homogeneously broadened. In inhomogeneously broadened samples, the destructive interference between the reradiated fields from the induced polarizations rather than T_2 determines the decay time constant. Therefore, roughly speaking, $1/T_2$ of Eq. (2) can be replaced by $1/T^*$ where $1/T^*$, is proportional to the inhomogeneous linewidth $\delta\omega$.

It is instructive to examine the effects of E_{II} or E_R on the time evolution of exciton population. E_{II} does not affect the time evolution of n, as can be readily seen by the optical Bloch equation

$$dn/dt + (1/T_1)n \propto \text{Im}(EP^*) , \quad (3)$$

where E is the electric field and P is the polarization, and T_1 is the longitudinal relaxation time. When only the δ-function-like incident field is included, i.e., $E = E_0 = \delta(t)$, the solution of Eq. (2) is simply, disregarding a proportionality constant, $n = \theta(t)$. Inclusion of E_{II} does not change this solution for $\text{Im}(E_{II}P^*) = 0$, since both E_{II} and P are 90° out of phase from E_0. However, E_R, which has the opposite sign from E_0, does have an effect on the exciton population. From Eqs. (1) and (3),

$$n = \theta(t')\{1 - (\alpha z/4)[1 - \exp(-2t'/T_2)]\} \quad (4)$$

assuming $T_1 \gg T_2$, which is well satisfied in semiconductors. In Fig. 2, the results of Eq. (4) are plotted for $\alpha z = 0.1$ (top), 0.5 (middle), and 1.5 (bottom). The appreciable initial population decrease shown in Fig. 2 is essentially caused by the fact that E_R is 180° out of phase from E_0.

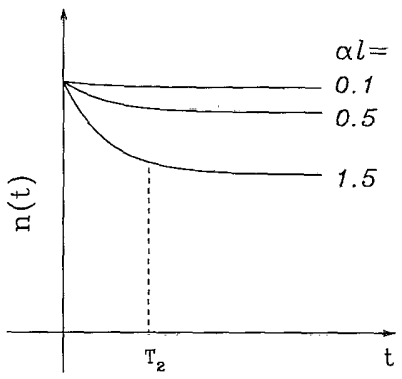

FIG. 2. Temporal evolution of the excitonic population resonantly excited by a δ-function pulse. From top to bottom, $\alpha l = 0.1$, 0.5, and 1.5. Only the first-order term from the optical Bloch equation for αl has been kept [Eq. (3)].

In this paper, we concentrate on how E_R causes pulse distortion and gives rise to interesting effects on both pump-probe and FWM experiments from GaAs quantum wells. The pulse distortion we study in this paper arises simply from linear absorption and should be distinguished from interesting results on pulse breaking effects for high-intensity pulses off resonance and at long propagation distances.[10,11] We studied the transmitted pulse shape near excitonic resonances using cross correlation in a nonlinear crystal [Fig. 3, with shutter (SH) out] in four different GaAs quantum-well samples with $l = 1700$ Å (sample A), 2550 Å (sample B), 6500 Å (sample C), and 6300 Å (sample D). The absorption linewidths of the heavy-hole (HH) resonances at 10 K are approximately, 0.7, 0.9, 4, and 1.8 meV for samples A, B, C, and D, respectively. In samples A and B, excitons are partially homogeneously broadened at 10 K whereas in samples C and D, they are predominantly inhomogeneously broadened. The experiments were performed at various temperature, excitation density, and detuning.

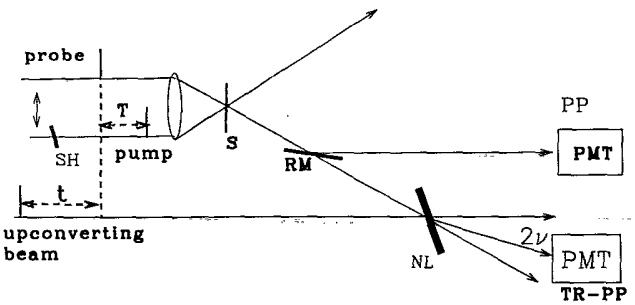

FIG. 3. Schematics for the experiments. SH, RM, NL, and PMT denote shutter, removable mirror, nonlinear crystal, and photomultiplier tube, respectively. T is the time delay between the pump and probe beams, whereas t acts as a real time measured from the arrival of the probe.

We found that the pulse distortion increases dramatically with increasing l, but it decreases with increasing dephasing rate (therefore, with increasing temperature or intensity) or inhomogeneous broadening of excitons.

We then *time-resolved* pump-probe experiments (Fig. 3, TR-PP) to study the effects of pulse distortion on pump-probe experiments. This offers a *complementary* way of performing the pump-probe experiments in "real time," rather than measuring the spectrally resolved (SR) or spectrally integrated (SI) signals as a function of time delay T. It is found that in thick samples, pump-induced change in the probe pulse shape results in interesting behavior of the TR-PP signal, both as a function of time delay and detuning. The effects of pulse distortion on time-resolved FWM were also studied. It is found that while samples A and B are little affected because of small pulse distortions, a distorted photon echo signal *whose temporal shape reflects the distorted pulse shape* is observed in the inhomogeneously broadened sample C.

To study both the phase and amplitude of the distorted pulse shape, a modified Michelson interferometer (Fig. 4) was used. It was found that at resonance, the distorted pulse has a well-defined node, around which the sign of the envelop function changes. When a slight detuning is introduced, the node is not well defined, and the wavelength of the transmitted pulse changes around the node, from the center laser wavelength to that of the exciton, unambiguously demonstrating that the pulse distortion is caused by the reradiation of induced exciton polarizations. Furthermore, we have performed an analytical calculation that shows how the excitonic population oscillates at the exit side of the sample where the pulse distortion is the largest.

This paper is organized in the following way. In Sec. II, we present a detailed investigation of pulse distortion in samples A, B, C, and D as functions of temperature, excitation density, and detuning. It is found that the distortion of pulse shape dramatically increases with l but decreases with increasing T_2 (thus with temperature or excitation intensity), inhomogeneous broadening, or detuning. In Sec. III, we concentrate on how pulse distortion affects the pump-probe or FWM experiment. The interferometric measurement and the analytical calculation on the time evolution of excitonic population subject to the distorted pulse shape are presented in Sec. IV and conclusions are offered in Sec. V.

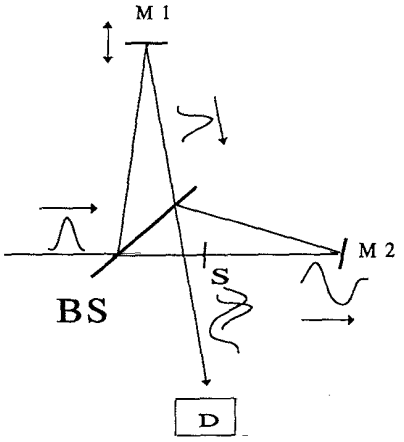

FIG. 4. A schematic for the modified Michelson interferometer; $M1$ and $M2$ mirrors: S, sample at 10 K. D, photodiode: and BS, beam splitter.

II. PULSE DISTORTIONS UNDER VARYING EXCITATION CONDITIONS

In this section, we probe the transmitted pulse shape by upconversion (see Fig. 3, with shutter in) under various excitation conditions on four GaAs multiple-quantum-well (MQW) samples with their substrates removed. The nominal well width (L_z) and periods (N) of these samples are 170 Å, 10 for sample A; 170 Å, 15 for sample B; 100 Å, 65 for sample C; and 84 Å, 75 for sample D. The relatively thin samples A and B have small linewidths (<1 meV), with FWM decay constant $\tau_{\text{decay}}=0.5$–0.75 ps at 10 K so that the homogeneous linewidth is bigger than 0.45 meV (Ref. 5) ($T_2=2\tau_{\text{decay}}$ for a homogeneously broadened line) whereas samples C and D are inhomogeneoulsy broadened at low temperatures (linewidth = 4 meV (C), 1.8 meV (D), $\tau_{\text{decay}}>2$ ps; $T_2=4\tau_{\text{decay}}$) and low density. A passively mode-locked, tunable Ti-Sapphire laser with 100–200-fs pulses (10–20-meV bandwidth) was used to perform transmission and pump-probe experiments at various temperatures, detuning, and photoexcitation densities (between 3×10^5 cm^{-2} and 3×10^{10} cm^{-2}).

Figure 5(a) shows the measured temporal shape of the

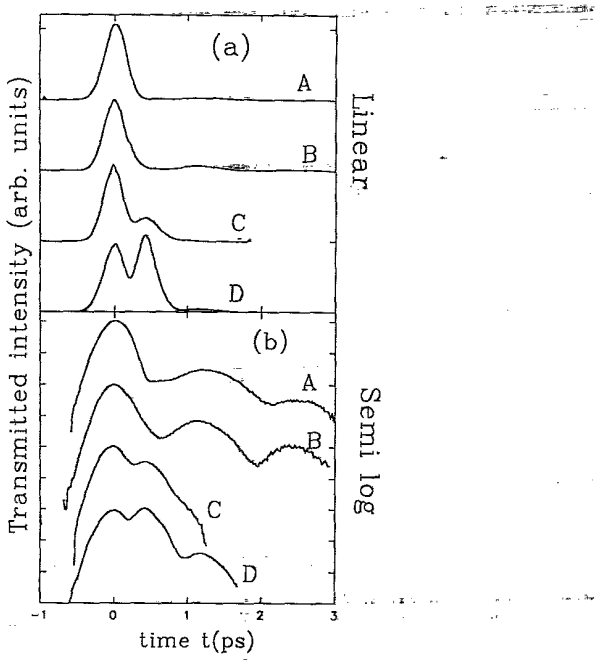

FIG. 5. (a) Transmitted intensity of the probe beam at low density and low temperature without the pump beam, from top to bottom, for samples A, B, C, and D. The laser is tuned to the heavy-hole excitonic resonance. (b) Semilogarithmic plot.

low-intensity probe pulse (in the absence of pump) after transmission through samples *A*, *B*, *C*, and *D* at 10 K, which are replotted in Fig. 5(b) in the logarithmic scale. The laser is tuned to the HH exciton resonance. In the linear scale [Fig. 5(a)], samples *A* and *B* show only small distortions, while samples *C* and *D*, particularly sample *D*, show much larger distortions. In the logarithmic plot [Fig. 5(b)], exponentially decaying tails that show well-defined "quantum beats" are evident for both samples *A* and *B*. The period roughly corresponds to the separations between the HH and light-hole (LH) excitons ($\approx$4 meV) in samples *A* and *B*. While the beating is a direct results of the large bandwidth of the laser exciting both HH and LH resonances simultaneously, the overall exponential decay of the small tail, which agrees well with that of FWM signal, is in agreement with the FID of induced polarizations (E_R), as described in Eq. (2).

Much thicker samples *C* and *D*, on the other hand, display *aperiodic oscillations that cannot be due to the* HH-LH *beat* since LH excitons in these samples are not excited or only very weakly excited because of large HH-LH separations ($\approx$10 meV for sample *C*, or $\approx$15 meV for sample *D*). Rather, they originate from the complicated interference between E_0 and E_R, which in turn can generate its own induced dipoles.[6-9] In bulk materials, the same aperiodic oscillation can be explained by the propagation of polaritons with different group velocities.[8] The decay constants of the transmitted pulses in these samples, despite the larger T_2's (determined by TI-FWM) are much smaller than samples *A* and *B*. This is because in these inhomogeneous broadened samples, the decay constant of the distorted pulse shape is determined not by T_2 but by the inhomogeneous broadening.

In Figs. 6(a) and 6(b) the effects of temperature on the pulse shapes are shown for samples *A* [Fig. 6(a)] and *D* [Fig. 6(b)]. In both samples, shorter dephasing times at 100 K (broken lines) make the distortions smaller. In sample *A*, the higher temperature essentially "cuts off" the FID tail, while in sample *D*, it makes the pulse distortion much smaller. This can be easily understood from Eq. (2), since for a given finite pulse width t_p, the effect of E_R on the pulse shape would become negligible when T_2 becomes comparable to t_p.

The effect of a high-intensity pulse (pump), which arrives at the sample at an earlier time, on the transmitted pulse shape, is presented in Fig. 7. This is especially relevant to the TR-PP experiments that we discuss in Sec. III. The transmitted pulse shapes, with (solid lines) or without (broken lines) a strong pump beam (2×10^{10} cm^{-2}) injected at an earlier time $t=-20$ ps, (therefore,

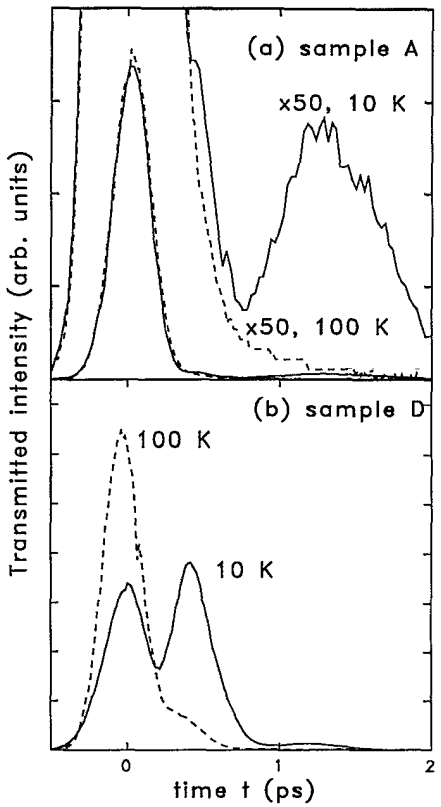

FIG. 6. Transmitted intensity of the probe at low density, at 10 (solid lines) and 100 K (broken lines) (a) for sample *A* and (b) for sample *D*. The laser is tuned to the heavy-hole resonance.

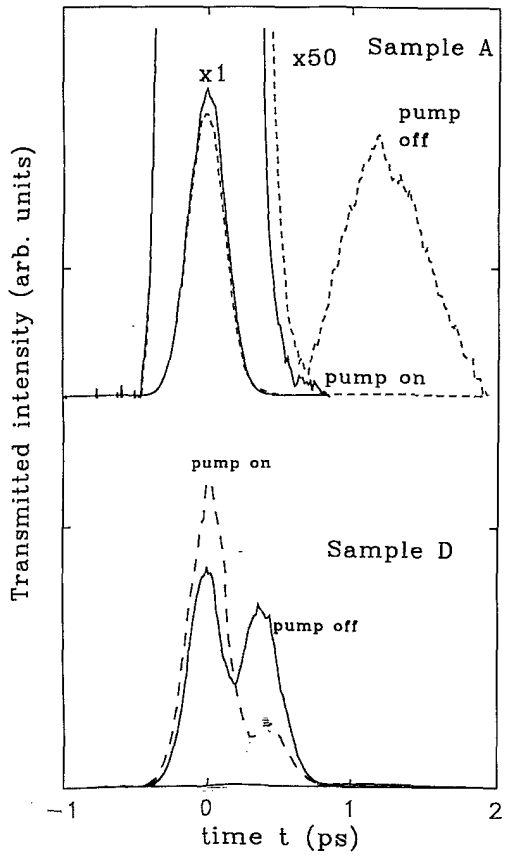

FIG. 7. Transmitted intensity of the probe with the pump beam on (dotted lines, 2×10^{10} cm^{-2}) and off (solid lines) at 10 K for sample *A* (top) and for sample *D* (bottom). Both samples are excited at the heavy-hole resonances.

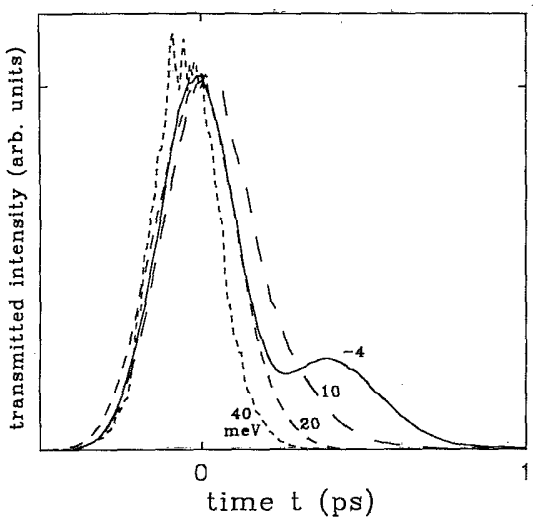

FIG. 8. Transmitted intensity of the probe for sample C at low density and temperature as a function of detuning from the heavy-hole exciton.

time delay $T=20$ ps), are shown for samples A (top) or D (bottom). It is clear that the effect of the pump beam on the probe beam is nearly identical with raising the temperature without the pump beam. This is because the free carriers and excitons introduced by the pump beam shortens the dephasing time of the excitons created by the probe beam dramatically.[12]

In Fig. 8, the transmitted pulse shape of sample C is plotted for several detunings from the HH excitons. As the laser is tuned away from the HH exciton, the pulse distortion becomes smaller. This can be easily understood when one considers *the transmitted laser spectrum.* At small detunings, the transmitted pulse spectrum shows a well-defined "dip" in the middle, whereas with increasing detuning, the transmitted pulse spectrum becomes less distorted. In time domain, this translates into smaller pulse distortion with increasing detuning from exciton resonance.

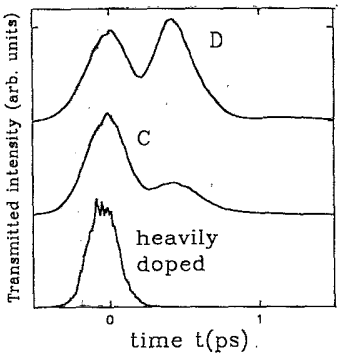

FIG. 9. Transmitted intensity of the probe beam at low temperatures and densities resonantly exciting inhomogeneously broadened samples with roughly the same l, either at heavy hole or at the Fermi edge. (Top) sample D with 1.8 meV of inhomogeneous broadening, (middle) sample C with 4 meV of inhomogeneous broadening, and (bottom) a heavily modulation-doped sample, which is intrinsically inhomogeneously broadened.

As we discussed in Sec. I, the inhomogeneous broadening reduces pulse distortion. In Fig. 9, the transmitted pulse shapes of C and D at 10 K, are compared with that of a heavily n-doped GaAs quantum-well sample (6×10^{11} cm^{-2}) with l of 6000 Å, resonantly excited at the Fermi edge. This sample, which has long dephasing times near the Fermi edge, is intrinsically inhomogeneously broadened with no excitonic features in absorption or photoluminescence excitation spectra.[13] Since these three samples have roughly the same l or T_2 but different inhomogeneous broadenings, its effect on pulse distortion can be isolated. The results in Fig. 9, which show decreasing pulse distortion with increasing inhomogeneous broadening, are in complete agreement with our prediction.

III. EFFECTS OF PULSE DISTORTION ON PUMP-PROBE OR FWM EXPERIMENTS

A. TR-PP experiments

In Sec. II, we discussed how the presence of strong pump pulse changes the temporal shape of the probe. In the simplest form of pump-probe experiments, the difference between the transmitted powers of the probe with or without a preceding pump beam is measured as a function of T without any experimental information on the spectral or temporal changes brought by the pump pulse. In other words, we measure the differential time-integrated change in the transmitted power P,

$$\frac{\Delta P}{P_0}(T)=\frac{\int[I_T(t)-I_0(t)]dt}{\int I_0(t)dt}, \tag{5}$$

without the detailed information on the pulse shapes $I_T(t)$ (with pump at time delay T) or $I_0(t)$ (without pump). Therefore, this simple PP experiment is both time and spectrally integrated. More detailed information can be obtained when the PP experiment is spectrally resolved (SR-PP), where the differential transmission spectrum is measured as a function of time delay. SR-PP has been widely used in semiconductors, and considerable insight into fundamental physical processes in semiconductors has been provided.[14–17] In SR-PP experiments near the exciton resonances, bleaching, broadening, and shift are identified as the main sources of signals.

In the following, we provide an alternative way of analyzing the PP experiment, which is to directly probe $I_T(t)$-$I_0(t)$ at a given time delay T using the upconversion technique (Fig. 3, TR-PP). In Fig. 10, the PP signal from sample B at 10 K with a pump intensity of $\approx2\times10^{10}$ cm^{-2} resonantly exciting the HH exciton is plotted as a function of T. At small negative time delays, the PP signal is negative (see inset), while around $T=0$, the coherent contribution, which essentially decays with a time constant $\approx T_2/2$ (T_2 measured from TI-FWM), is evident. For $T>0$, the PP signal is positive (bleaching). It is instructive to time resolve this experiment to understand the origin of the PP signal, particularly when it is

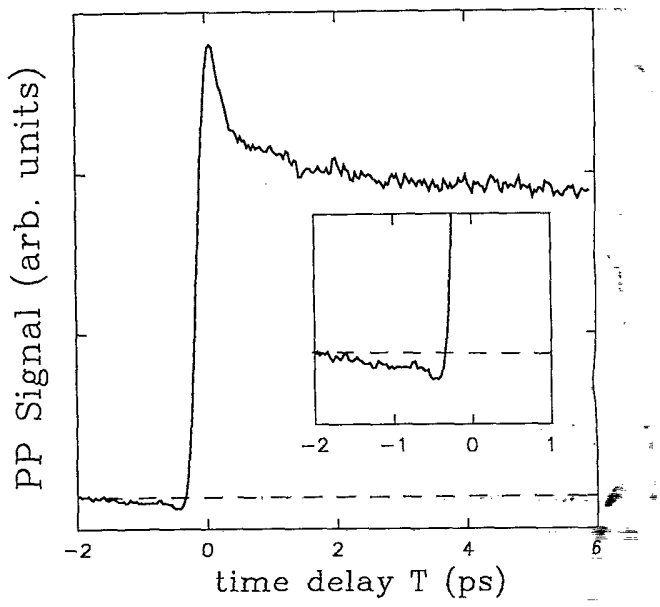

FIG. 10. Pump-probe signal (TI-PP, 2×10^{10} cm^{-2}) as a function of T for sample B under resonant excitation at 10 K. At much of the negative time delay, the differential transmission is negative whereas at positive time delays, it is bleaching (positive). Inset: blowup of the region showing mostly negative TI-PP.

negative.

In Fig. 11, normalized TR-PP signals are plotted against t measured from the peak position of the probe beam, for $T=-0.5$ (thus, the pump beam arriving at $t=0.5$ ps), -0.2, and 6 ps (thus pump beam arriving at $t=-6$ ps). At $T=6$ ps, TR-PP is positive (bleaching)

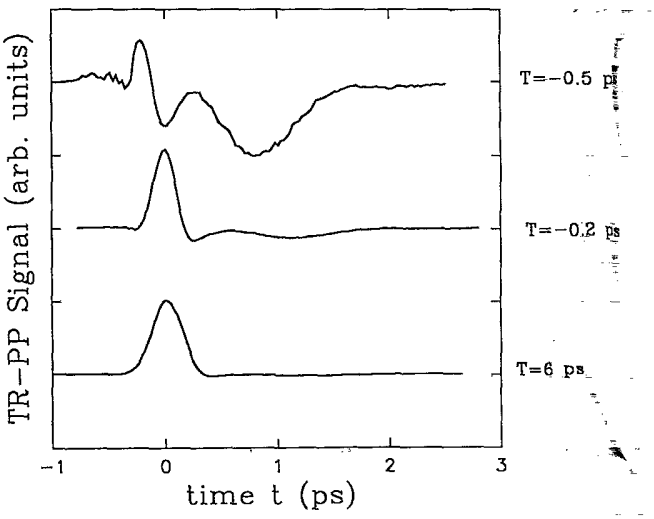

FIG. 11. Normalized TR-PP at various time delays under the same conditions as Fig. 10. Time delays are, from top to bottom, -0.5, -0.2, and 6 ps. Note that at -0.5 ps, TR-PP is dominated by the negative signal that is a direct result of pulse distortion.

and resembles autocorrelation of the incident pulse shape, although closer look reveals small negative contribution at small positive times. This is more or less what one expects when the sample is assumed to be infinitesimally thin, and also in agreement with relatively small pulse distortion in this sample. However, at $T=-0.5$ ps, the signal is mostly negative and occurs after $t=0.5$ ps, which is when the pump beam arrives. Apart from the interesting oscillations, TR-PP at $T=-0.5$ ps can be understood by realizing that the part of the probe affected most by the pump beam that arrives later is the FID part, which is cut off by the strong pump beam that arrives at $t=0.5$ ps and reduces T_2 of excitons. In principle, there would be no signal before $t=0.5$ ps, for the temporal evolution of the probe cannot be affected until the probe beam arrives! On the other hand, time integration of the TR-PP signal at $T=-0.5$ ps up to $t=0.5$ ps is nearly zero because the positive and negative parts mostly cancel. While more studies are needed to understand this interesting phenomenon, the pump-induced cut off of the FID of the probe is identified as the main cause for the negative PP signal at negative time delays.

In the literature, the so-called perturbed FID has been identified as the main source of the oscillating (in frequency) SR-PP signal at negative time delays.[14–17] This signal is essentially a coherent, sinusoidal modulation (in the frequency domain) of the FID of the probe beam by the electric field of the pump beam. As such, the net, spectrally integrated signal is zero. Theoretically, the perturbed FID is derived assuming that T_2 is not affected by the preceding pump beam, and with an implicit assumption of an infinitely thin sample. With these simplifying assumptions, it was shown that the net SI signal is zero and the contribution disappears at positive time delays.

Unlike the perturbed FID of the literature, the net negative signal we observe at negative time delays result from the change in T_2 of excitons caused by the strong pump beam. Therefore, this effect is essentially "thermal" and exists in positive time delays as well, as shown in Fig. 7 of Sec. II. This is precisely the origin of the relatively small negative TR-PP signals for $T=6$ ps (Fig. 11) that occur after the strong bleaching signal. The relative importance of this net negative contribution to TR-PP would disappear in an infinitesimally thin sample and would increase rapidly with increasing l. It should be reminded that the absolute strength of the "small" negative TR-PP signal at $T=6$ ps is larger than the one shown at $T=-0.5$ ps where the bleaching does not exist. The effect of change in T_2 caused by the pump beam should also be present in the SR-PP experiments (broadening). However, the spectrally oscillating perturbed FID signal, combined with the inhomogeneous broadening and the ac stark effect make this effect difficult to be isolated. Our TR-PP experiments provide a complementary way of performing PP experiments where the effect of changing T_2 brought by the pump beam is easily identified as a source of the PP signal.

Thus far, we discussed the results from the relatively thin sample B. At positive time delays, TR-PP could be

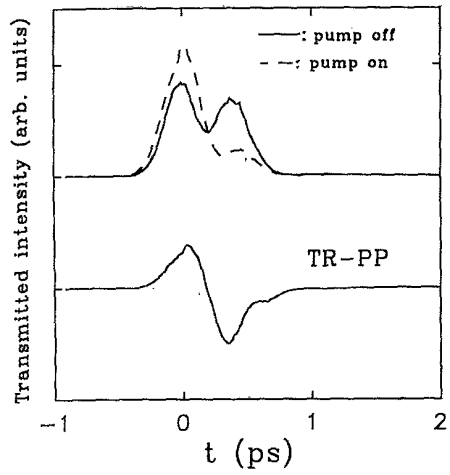

FIG. 12. Transmitted pulse intensity at 10 K for sample *D*, with (broken lines) or without (solid lines) strong pump beam. The subtraction between these two curves constitutes the TR-PP signal.

easily interpreted as a strong bleaching followed by the much weaker negative signal originating from cut off of FID. In sample *D* where the pulse distortion is the largest, TR-PP shows a negative signal, which is almost as strong or even stronger than the positive, bleaching signal, as shown in Fig. 12. This is simply because the large pulse distortion makes the cutoff of FID, or the contribution of pulse distortion to TR-PP comparable to or larger than the positive, bleaching signal. In the following, we show that the relative strength of the negative TR-PP signal is not simply determined by the amount of pulse distortion at low intensity, but also by the amount of change in T_2 induced by the pump. In Fig. 13(a), the transmitted pulse shapes in sample *C* are plotted at various detunings from the HH exciton, where with the increasing detuning, the pulse distortion becomes smaller. The corresponding TR-PP are shown in Fig. 13(b). It is interesting to note that the relative strength of the negative signal is the largest for the detuning of 10 meV, where the pulse distortion is much smaller than that for the detuning of −4 meV. This is because at 10 meV of detuning, far more free carriers are created so that the change in T_2 is much larger than at −4 meV of detuning, confirmed by FWM experiments.[12] Therefore, the resulting negative signal can still be larger than the bleaching signal despite the relatively small pulse distortion. Even at 20 or 40 meV of detuning, the existence of a negative TR-PP signal is clearly visible.

It is clear that in samples *C* and *D*, the simple analytical Eq. (2) appropriate for $\alpha l < 1$ does not apply. This is because higher-order terms in αl begin to contribute to the pulse distortion, which means that the incident field at a position z_0 is no longer the δ-function pulse alone. Rather, the δ-function pulse combined with the reradiation of the induced dipoles at $z < z_0$ act as the incident field. In two-level systems of bulk materials, resonant pulse propagation at low densities can be solved more or less exactly by coupled Maxwell-Bloch equations that relate the electric field, the induced polarization, and the exciton population, with T_2, detuning and oscillator strength as parameters.[6,7] While such equations gives rise to Eq. (3) in the limit of $\alpha l < 1$, in general, the solution is somewhat complicated, although it results in a closed integral form,[6,7] and can be solved numerically. It is important to note that the concept of classical polariton is inherent in these coupled equations, and it arises from the coupled nature of the equations, for the exciton polariton is simply a coupled system of electric field and the excited two-level system.

In semiconductor quantum wells, the purely analytical approach used in bulk materials is difficult since the wells are separated by finite barriers. Furthermore, excitons cannot always be viewed as a two-level system and, in general, semiconductor Bloch equation should be used to describe exciton dynamics. Therefore, to understand our results quantitatively, we have performed calculations using microscopic coupled Maxwell-semiconductor Bloch equations.[18] In this approach, semiconductor Bloch equations are solved for the first well with the input pulse as a source, whose solution (the induced polarization) enters the Maxwell equations. The resulting electric field, which is slightly distorted (due to reradiation of induced polarization), enters the next well to become the source of

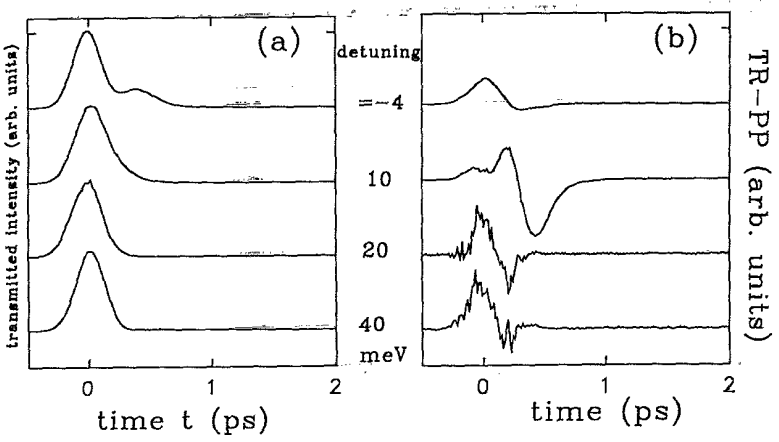

FIG. 13. (a) Pulse distortion of a low-intensity probe at various detunings (from top to bottom, −4, 10, 20, and 40 meV) for sample *C*. (b) Corresponding TR-PP.

the semiconductor Bloch equations, and so on. Polariton effects are again inherent in this approach: If we assume that the barrier thickness goes to zero and, therefore the material becomes bulk, classical polariton results.

Some of the results of the coupled Maxwell-semiconductor Bloch equations were previously reported by us,[19] and they correctly reproduce the main features of our experimental results such as the aperiodic oscillations of sample D [Fig. 5(b)] or the effect of reduced T_2 (330 fs) on the pulse shape [Figs. 6(a), 6(b), or 7].

B. TR-FWH experiments

In this section we study the effects of pulse distortion on TR-FWM (Fig. 14) from sample C where significant pulse distortion exists. In Figs. 15(a) and 15(b), we show TR-FWM of sample C at 10 K and at relatively low density (2×10^9 cm^{-2}), tuned slightly below HH exciton for the cross-polarized [Fig. 15(b)] and collinearly [Fig. 15(a)] polarized geometries. To simplify the discussion, we denote the primary and the secondary peaks of the distorted pulse (broken lines) α and β, respectively. At a time delay $T>0$, the first pulse arrives at $t=-T$, and the second beam arrives at $t=0$. In both polarization geometries, the signatures of photon echo are clear in Figs. 15(a) and 15(b): the peak occurs roughly at $t\approx T$. This is consistent with the inhomogeneous broadening of this sample at low temperature (linewidth ≈4 meV, $T_2\approx10$ ps determined from FWM). Furthermore, the distorted pulse shape is reflected in the shape of the echo signals, with peaks α and β readily identifiable. Therefore, from an experimental point of view, the influence of the pulse distortion in TR-FWM is more or less equivalent to performing the experiment with an already distorted pulse in a thin sample.

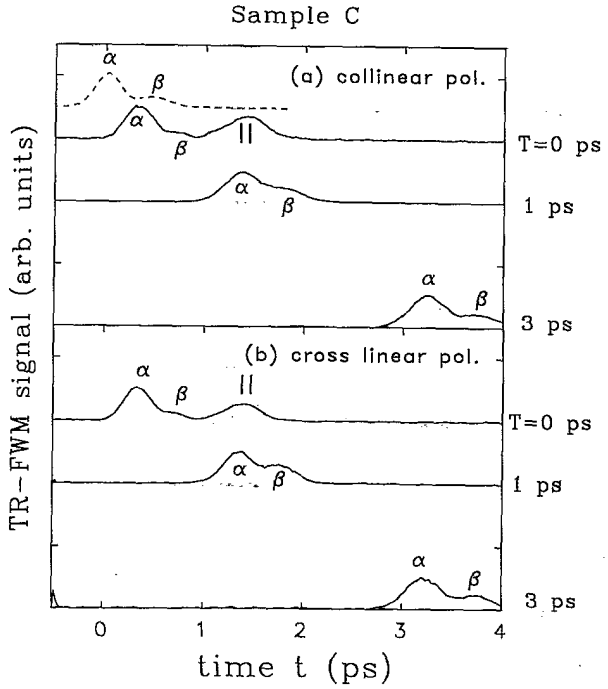

FIG. 15. TR-FWM from sample C in (a) the collinearly polarized geometry and (b) the cross linearly polarized geometry. The distorted pulse shape is denoted as broken lines, with α and β denoting the primary and the secondary peaks, respectively. The detuning is -4 meV and the density is estimated to be 3×10^9 cm^{-2}.

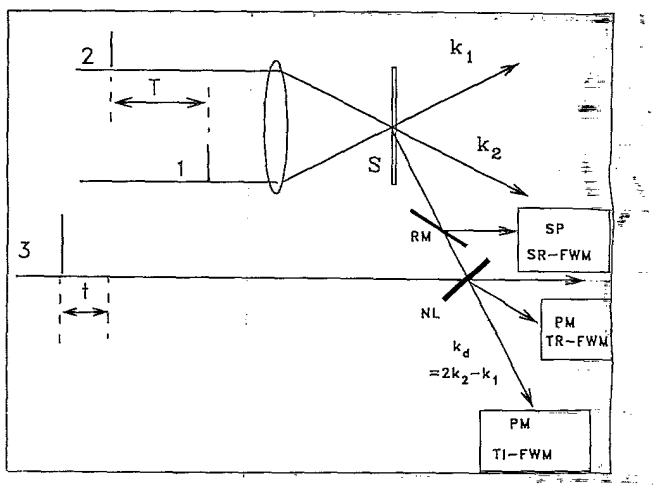

FIG. 14. Schematics for TR-FWM, along with those of TI and SR-FWM. In TR-FWM, the diffracted signal in the direction of k_d is upconverted in NL crystal with a third beam. The time delay thus introduced (t) acts as a real time, so that time evolution of FWM signal at a fixed time delay (T) can be probed. S, SP, RM, and PM denote sample, spectrometer, removable mirror, and photomultiplier tube, respectively.

At $T=0$, an additional peak at $t\approx1.4$ ps is clearly visible in both polarizations. Since both pulses, which arrive at $t=0$, have completely passed through the sample at $t\approx1.4$ ps, we identify this peak as the signal due to the diffraction of interaction-induced (II) field. In the high-quality sample A, such a delayed II signal completely overshadowed the prompt signal (free induction decay of the laser field) at all time delays.[5] In this sample C, the II signal is comparable to the prompt signal at $T=0$, while photon echo reflecting the pulse shape dominates FWM at $T=1$ and 3 ps. This can be readily understood by noting that, in general, the effect of inhomogeneous broadening is to multiply the TR-FWM shape (without such inhomogeneous broadening) by a Gaussian $\exp[-(t-T)^2/T^{*2}]$ where T^* is inversely proportional to the inhomogeneous broadening.[1-5] At $T>T^*$, FWM is dominated by the photon echo that peaks at $t\approx T$, whereas at $T=0$, the Gaussian $\exp(-t^2/T^{*2})$ suppresses the delayed II signal relative to the prompt signal that peaks near $t=0$. While detailed discussion of TR-FWM will be published elsewhere, it is clear that the information on the pulse shape is vital to the interpretation of TR-FWM experiments. In other words, without analyzing the transmitted pulse shape, it would have been difficult to interpret the additional peaks in TR-FWM from this sample.

IV. INTERFEROMETRIC MEASUREMENTS

In this section, we discuss the interferometric measurements performed on sample *D*. We put the sample in one arm of a modified Michelson interferometer so that the interference pattern is obtained between the nondistorted pulse and the pulse that is distorted as a result of passing through the sample (Fig. 4). The resulting pattern would closely resemble the actual envelope function of the distorted pulse. Figure 16 shows the interference pattern between the original and the distorted pulses for sample *D* resonantly excited at the HH resonance at 10 K (top) and 100 K (bottom). At 10 K, two nodes at 0.12 and 0.7 ps are clearly visible, whereas at 100 K (bottom), the nodal position shifts toward longer time delay (0.2 ps), and the pulse distortion becomes smaller. These results are consistent with the results of Fig. 6(b), but are much more pronounced. Closer examination of the nodal regions at both temperatures shows the change of sign of the envelope function, as had been demonstrated by the 108° change of phase around the node in an earlier work.[19]

A slight detuning of the laser from the resonance (Fig. 17) shows that a well-defined node does not occur and the nodal region becomes thicker with increasing detuning. This is because the rear part of the pulse has the frequency of the exciton resonance whereas the frequency of the frontal part is determined by the center laser frequency. Because of this difference in center frequency, perfect cancellation is not possible. These results unequivocally demonstrate that the origin of the pulse distortion is the reradiation from the induced polarization.

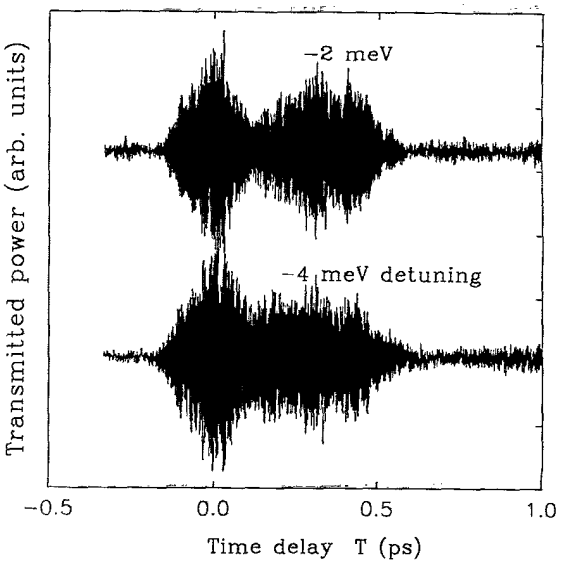

FIG. 17. Interference pattern as a function of detuning showing the disappearance of a well-defined node with increasing detuning. The detunings are −2 (top) and −4 meV (bottom).

One interesting question concerns the effect of this interesting pulse shape on the time evolution of the excitonic population. In sample *D*, excitons at the exit side of the sample are subject to an electric-field envelope function that is oscillating aperiodically, as illustrated in Fig. 18 (top), which shows an envelope function loosely resembling the results of Fig. 16 at 10 K. The resulting induced polarization, which is essentially an integral in time of the electric-field envelope function, is plotted in the middle of Fig. 18. From the optical Bloch equation

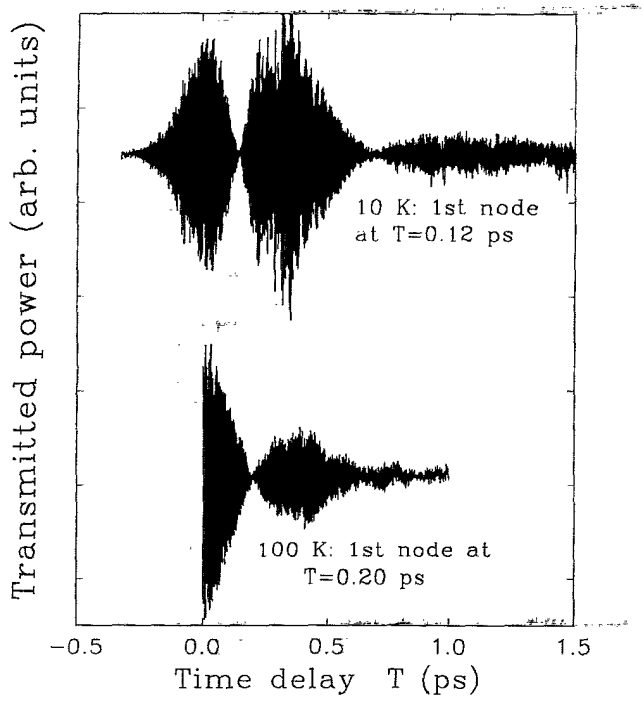

FIG. 16. Interference pattern between the transmitted beam through the sample *D* and the original one at 10 (top) and 100 K (bottom).

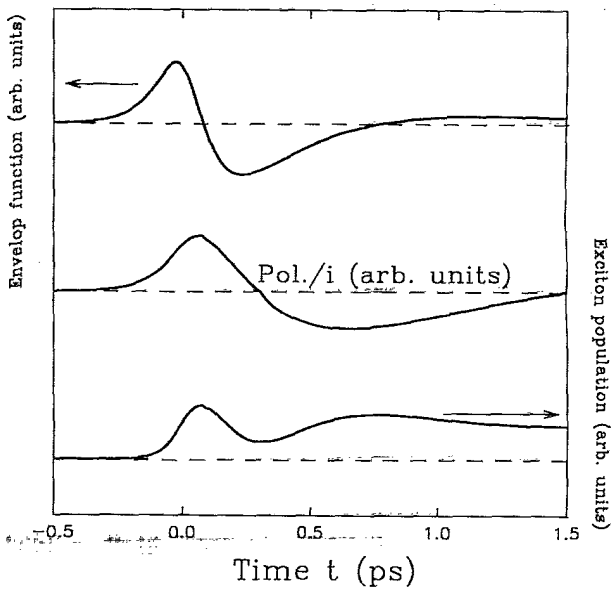

FIG. 18. Theoretical calculation assuming a two-level system to fit the interference pattern of Fig. 16. Top, envelope function of the electric field; middle, polarization; bottom, the excitonic population as a function of time.

[Eq. (3)] assuming $T_1 = \infty$, the time evolution of excitonic population can be calculated and the results are shown at the bottom, where the excitonic population oscillates aperiodically.

V. CONCLUSIONS

In conclusion, we have studied femtosecond pulse distortion in GaAs quantum wells under wide ranges of excitation conditions and sample parameters. We found that the pulse distortion is a strong function of l, temperature, density, detuning, and inhomogeneous broadening. This distortion comes from the interference between the laser field and the reradiated field of the induced dipoles, confirmed by interferometric measurements. Since the pulse distortion depends strongly on the dephasing time, the pump-induced change in the dephasing time is an important factor in pump-probe experiments, and leads to net induced absorption for moderately thick (>6000 Å) quantum wells. These results are in good agreement with microscopic, Maxwell-semiconductor Bloch-equation calculations. In TR-FWM, the shape of the photon echo from an inhomogeneously broadened sample is modified accordingly due to pulse distortion. Our results show that pulse distortion effects must be considered carefully in the interpretation of pump-probe and other femtosecond experiments, especially when $l > 3000$ Å in the vicinity of excitonic resonance at low temperatures.

ACKNOWLEDGMENTS

We thank J. P. Gordon, E. P. Ippen, W. H. Knox, P. Planken, and P. Y. Yu. for helpful discussions.

*Present address: Department of Physics, Seoul National University, Seoul, Korea.

[1]C. Stafford, S. Schmitt-Rink, and W. Schäfer, Phys. Rev. B **41**, 10 000 (1990).

[2]W. Schäfer, F. Jahnke, and S. Schmitt-Rink, Phys. Rev. B **47**, 1217 (1993).

[3]K. Leo, M. Wegener, J. Shah, D. S. Chemla, E. O. Göbel, T. C. Damen, S. Schmitt-Rink, and W. Schafer, Phys. Rev. Lett. **65**, 1240 (1990).

[4]M. Wegener, D. S. Chemla, S. Schmitt-Rink, and W. Schäfer, Phys. Rev. A **42**, 5675 (1990).

[5]D. S. Kim, J. Shah, T. C. Damen, W. Schäfer, F. Jahnke, S. Schmitt-Rink, and K. Köhler, Phys. Rev. Lett. **69**, 2725 (1992).

[6]H.-J. Hartmann and A. Laubereau, J. Chem. Phys. **80**, 4663 (1984).

[7]A. Laubereau and W. Kaiser, Rev. Mod. Phys. **50**, 607 (1978).

[8]D. Fröhlich, A. Kulik, B. Uebbing, A. Mysyrowica, V. Langer, H. Stolz, and W. von der Osten, Phys. Rev. Lett. **67**, 2343 (1991).

[9]A. Puri and J. L. Birman, Phys. Rev. A **27**, 1044 (1983).

[10]P. A. Harten, A. Knorr, J. P. Sokoloff, F. Brown de Colstoun, S. G. Lee, R. Jin, E. M. Wright, G. Khitrova, H. M. Gibbs, S. W. Koch, and N. Peyghambarian, Phys. Rev. Lett **69**, 852 (1992).

[11]S. W. Koch, A. Knorr, R. Binder, and M. Lindberg, Phys. Status Solidi B **173**, 177 (1992).

[12]D. S. Kim, J. Shah, J. E. Cunningham, T. C. Damen, W. Schäfer, M. Hartmann, and S. Schmitt-Rink, Phys. Rev. Lett. **68**, 1006 (1992).

[13]D. S. Kim, J. Shah, J. E. Cunningham, T. C. Damen, S. Schmitt-Rink, and W. Schäfer, Phys. Rev. Lett. **68**, 2838 (1992).

[14]C. H. Brito Cruz, J. P. Gordon, P. C. Becker, R. L. Fork, and C. V. Shank, IEEE J. Quantum Electron. **24**, 261 (1988).

[15]W. H. Knox, in *Hot Carriers in Semiconductors Nanostructures*, edited by J. Shah (Academic, Boston, 1992).

[16]R. Binder, S. W. Koch, M. Lindberg, W. Schäfer, and J. Jahnke, Phys. Rev. B **43**, 6520 (1991), and references therein.

[17]M. Joffre, D. Hulin, A. Migus, and A. Antonetti, C. Benoit à la Guillaume, N. Peyghambarian, M. Lindberg, and S. W. Koch, Opt. Lett. **13**, 276 (1988).

[18]W. Schäfer and K. Henneberger, Phys. Status Solidi B **159**, 59 (1990).

[19]D. S. Kim, J. Shah, D. A. B. Miller, T. C. Damen, W. Schäfer, and L. N. Pfeiffer, Phys. Rev. B **48**, 17 902 (1993).